European Review for Medical and Pharmacological Sciences 2019; 23: 8588-8597

Role of miR-133a in regulating TGF-β1 signaling pathway in myocardial fibrosis after acute myocardial infarction in rats

B.-T. YU[1], N. YU[2], Y. WANG[3], H. ZHANG[1], K. WAN[1], X. SUN[1], C.-S. ZHANG[1]

[1]Department of Emergency, The Affiliated Central Hospital of Qingdao University, Qingdao, China
[2]Department of Cardiovascular Medicine, The First People's Hospital of Jinan, Jinan, China
[3]International Components for Unicode, The Affiliated Central Hospital of Qingdao University, Qingdao, China

Abstract. – OBJECTIVE: The aim of this research was to explore the effect of microRNA-133a (miR-133a) on myocardial fibrosis and cardiac function after myocardial infarction in rats, and to investigate the possible regulatory mechanism.

MATERIALS AND METHODS: Myocardial infarction model was successfully established in rats by ligation of the left anterior descending coronary artery. After miR-133a overexpression in rats myocardium, cardiac function was examined by echocardiography. Meanwhile, the degree of myocardial fibrosis was detected by Masson staining. In addition, the expression of α-smooth muscle actin (α-SMA) in cardiomyocytes was detected by immunohistochemistry. Quantitative Real-time polymerase chain reaction (qRT-PCR) was performed to analyze the expression level of miR-133a in the junction of myocardial infarction. The mRNA expressions of transforming growth factor-β1 (TGF-β1), connective tissue growth factor (CTGF), collagen type 1 (col 1), collagen type 3 (col 3) and α-SMA were measured by qRT-PCR as well. Furthermore, the protein levels of the above genes were detected by Western blotting.

RESULTS: MiR-133a expression in the infarct border zone of myocardial tissue was significantly decreased on the 28th day after myocardial infarction surgery ($p<0.05$). In addition, up-regulation of miRNA-133a in myocardial tissue of rats with myocardial infarction could remarkably improve cardiac function and reduce collagen volume fraction. Furthermore, the mRNA and protein expression levels of TGF-β1, CTGF, col1, col3, α-SMA in myocardial tissue were obviously decreased after miRNA-133a up-regulation ($p<0.001$).

CONCLUSIONS: Overexpression of miR-133a down-regulates the mRNA and protein levels of TGF-β1 and CTGF after myocardial infarction. Moreover, this may eventually reduce myocardial collagen deposition, inhibit myocardial fibrosis and improve cardiac function.

Key Words:
Acute myocardial infarction, MiR-133a, Myocardial fibrosis, TGF-β1.

Introduction

Myocardial infarction (MI) is a cardiovascular disease that seriously endangers human health. It can eventually lead to poor prognosis, such as heart failure. Myocardial fibrosis (MF) is an important pathophysiological change after MI. Cell interstitial hyperplasia will be induced by the activation of various fibrosis-related factors[1]. MF can lead to increase cardiac stiffness, decreased diastolic function, changes in normal cardiac electrophysiological structures to induce arrhythmias, and even sudden death[2,3]. Therefore, inhibition of MF is of great importance for preventing heart failure caused by MI. Abnormal accumulation of collagen fibers in myocardial tissues can result in obviously increased collagen concentration in the myocardium or an increase in collagen volume fraction (CVF). Various types of collagen disorder and imbalance in proportion are called MF[4]. The development of MF is affected by multiple factors, including immune system, body cytokines and RAAS system. However, the mechanisms of different types of MF are not identical. At the same time, the formation mechanism of MF can also regulated by various factors, such as angiotensin, endothelin, nitric oxide, transforming growth factor, connective tissue growth factor and intracellular calcium. On the whole, the imbalance of synthesis, metabolism and degradation of myocardial extracellular matrix

Corresponding Author: Chengsen Zhang, MM; e-mail: zcsys@163.com

collagen leads to the occurrence of MF[5,6]. MicroRNA (miRNA) is a type of single-stranded small RNA with about 18-25 ribonucleotides in length. The main function of miRNA is to regulate basic processes of human life activities, such as cell growth, proliferation and differentiation, as well as cell apoptosis, aging, death, etc.[7]. In recent years, studies have found that miRNAs regulate the expressions of cardiovascular disease-related genes, such as miR-1, miR-21, miR-133, miR-208, etc. Meanwhile, they are also widely involved in pathophysiological processes of cardiovascular diseases, including MF, cardiac hypertrophy, and arrhythmia[8]. MiR-133a is one of the most abundant miRNAs in the heart. It plays an important role in the regulation of cardiac development, such as cardiomyocyte differentiation and proliferation[9]. Previous studies have focused on the effect of miR-133 on cardiac development. For example, miR-133a promotes the differentiation and proliferation of embryonic stem cells into myoblasts, whereas inhibits the differentiation of myoblasts into cardiomyocytes. Therefore, any abnormality in the expression of miR-133a during embryonic stage will affect the normal development of the heart[10]. It has been found that in miR-133a-deficient mice, cardiac structural abnormalities, such as ventricular septal defect, cardiac enlargement and ventricular wall thinning, are accompanied by severe MF and heart failure[11,12]. These findings indicate that miR-133a is essential in maintaining the balance of heart extracellular matrix. In a variety of cardiac hypertrophy pathology models, the expression of myocardial miR-133a is significantly decreased. Meanwhile, up-regulation of miR-133a can greatly improve pathological processes such as cardiac hypertrophy. Therefore, miR-133a may serve as a cardio-protective factor[13]. Transforming growth factor-β1 (TGF-β1) and connective tissue growth factor (CTGF) are important pro-fibrotic factors. As a promoter of fibrosis, TGF-β1 can induce CTGF production. Meanwhile, CTGF acts as a downstream mediator of TGF-β1 to promote its fibrosis[14]. Both of the two molecules can promote the phenotypic transformation of fibroblasts. They can also induce the synthesis of extracellular matrix components, such as collagen, proteoglycan and laminin, through various pathways[15]. In this study, we found that miR-133a played its role by regulating the expression of genes closely related to fibrosis[16,17]. In nicotine-induced canine atrial fibroblasts, the expression level of miR-133a is decreased. This may result in increased synthesis of TGF-β1, accompanied by massive collagen synthesis[18]. High expression of CTGF in hypertrophic ventricular myocytes is also associated with decreased expression of miR-133 in various animal models of cardiac hypertrophy[19]. In this work, a rat model of MI was successfully constructed by ligating the anterior descending coronary artery. The effect of miR-133a overexpression on the transcription and translation of TGF-β1 and CTGF, as well as the regulation of MF were observed. In addition, we investigated the role and mechanism of miR-133a in MF after MI.

Materials and Methods

Animal Grouping

A total of 60 healthy male Sprague-Dawley (SD) rats were fed in a specific-pathogen-free (SPF) environment in (20 ± 2)°C, with 60% to 70% of relative humidity and light and dark in turn. According to the random number table method, all SD rats were randomly divided into 3 groups, including: sham operation group (no ligation after crossing the line), control group (ligation and intra-cardiac injection of phosphate-buffered saline (PBS)), and miR-133a up-regulation group (ligation and intra-cardiac injection of miR-133a precursor). 20 rats were included in each group. This study was approved by the Animal Ethics Committee of Qingdao University Animal Center.

Animal Model Preparation

Rats were first anesthetized by intraperitoneal injection of 10% chloral hydrate at a dose of 350 mg/kg. The supine position was fixed on the operating platform, and tracheal intubation assisted ventilation. The skin in the anterior region was routinely prepared and disinfected. Subsequently, the skin was cut longitudinally at the most obvious point of the heartbeat. After separation and fully expose, the left ventricle was injected with PBS or miR-133a precursor. At the same time, non-invasive vascular clamp was used to gently clamp the ascending aorta for about 10s. Immediately after the heart rate slowed down, the vascular clamp was released. If there was no sign of death after 10 min, the left anterior descending coronary artery was ligated between the left atrial appendage and the pulmonary artery. After ligation, the left ventricular wall became pale,

the wall motion was weakened, and ST period in electrocardiograph (ECG) was raised. Then the model was confirmed successfully established in rats. In the sham operation group, the needle was surgically sutured at the same site. However, the left anterior descending coronary artery was not ligated. The thoracic cavity was closed layer by layer, and the chest skin wound was applied with cotton swab penicillin sodium powder after surgery. Single cage was fed freely at room temperature. Each rat was given intraperitoneal injection of 100,000 units/day penicillin for anti-infection three days after operation.

Echocardiography

On the 28th day after surgery, the rats were intraperitoneally injected with 4% chloral hydrate (0.65 mL/kg) and fixed in supine position. The chest hair was then sheared. Echocardiography (probe 10 S, image depth 2.0-4.0 cm, frequency 11.4 MHz) was used to check left ventricular end-diastolic diameter (LVEDD), left ventricular end-systolic diameter (LVESD), left ventricular fractional shortening (LVFS) and left ventricular ejection fraction (LVEF).

Specimen Collection and Processing

After the completion of echocardiography in each group, the rats were sacrificed. Cardiac specimens were dissected, and myocardial tissue at the junction of MI was collected. After washing with pre-cooled saline, part of the tissues were frozen in -80°C for subsequent use. Meanwhile, the other part of the tissues were immediately soaked in 4% paraformaldehyde. Paraffin-embedded sections were then prepared for pathological examination.

Masson Staining

Myocardial tissue was first fixed in 4% paraformaldehyde, washed, dehydrated and immersed in wax. Then the tissues were embedded, cut into 4 μm slices and placed in a warm water dish. Unfolded tissue sections were placed on a glass slide and incubated at room temperature for 60 minutes. After staining with Masson, the sections were observed under a microscope. In Masson stained sections, cardiomyocytes were stained red. However, collagen fibers were stained as a blue strip or homogeneous structure, which were located in the intercellular space. Lastly, collagen volume fraction (CVF) was calculated using Image-Pro Plus software (Silver Springs, MD, USA).

Immunohistochemistry

Tissue sections were digested with xylene and dehydrated with alcohol. Antigen was extracted from α-smooth muscle actin (α-SMA) slide. The primary antibody was added dropwise, followed by incubation at 4°C overnight. Next, the slides were washed with PBS and incubated with corresponding secondary antibody at 30°C for 30 min. Afterwards, the antigen was developed by diaminobenzidine (DAB) (Solarbio, Beijing, China). After counterstaining with hematoxylin, the antigen was differentiated by hydrochloric acid alcohol, sealed by gum and observed under a microscope. The positive and negative indicator of immune response showed brown and blue in the nucleus, respectively. 10 fields of view were randomly selected from each sample, and 100 nuclei were counted continuously. Finally, the number of positive cells was recorded, and the positive rate was calculated.

Western Blotting Assay

Myocardial tissue was first washed with pre-cooled physiological saline solution at 4°C and then minced. An appropriate ratio of radioimmunoprecipitation assay (RIPA) lysate (Beyotime, Shanghai, China) was added for lysis. After homogenization, the supernatant was centrifuged, and the concentration of total protein was determined according to the instructions of bicinchoninic acid (BCA) assay kit (Pierce, Rockford, IL, USA). Western blotting was used to detect the expressions of proteins, including TGF-β1, CTGF, collagen type 1 (col 1) and collagen type 3 (col 3).

Quantitative Real-Time Polymerase Chain Reaction (qRT-PCR)

Total RNA in rat myocardial tissues was extracted according to the kit instructions (TaKaRa, Otsu, Shiga, Japan). Extracted RNA was reverse transcribed into complementary deoxyribose nucleic acid (cDNA) in strict accordance with kit instructions (TaKaRa, Otsu, Shiga, Japan). The mRNA sequences of miR-133a, TGF-β1, CTGF, col 1, col 3, α-SMA and glyceraldehyde 3-phosphate dehydrogenase (GADPH) were searched from Gen Bank. GAPDH was used as an internal reference. Primers were designed using Primer 5.0 software. The mean Ct values of target genes and reference genes were determined by qRT-PCR. The expression of genes of treatment group relative to blank group was calculated by the $2^{-\Delta\Delta Ct}$ method. Primer sequences used in this study were as follows:

TGF-β1, F: 5'-CCACCACGCTCTTCTGTC-TACC-3', R: 5'-CTGGCTACGGGCTTGTCA-3'; miR-133a, F: 5'-CTGCAGCTGGAGAGTGTG-CG-3', R: 5'-GTGCTCTGGAGGCTAGAGGT-3'; CTGF, F: 5'-AGCAGCGGCATTTGGACAA-3', R: 5'-CGTGCGAATAGCGACAGTTCT-3'; col 1, F: 5'-GCTTTCAACACGCATG-3', R: 5'-AACTGCACCTGTACGATCG-3'; col 3, F: 5'-ACATAAAGACATGAA-3', R: 5'-CTTTCAACACGCAGGACAGAT-3'; α-SMA, F: 5'- CAGAGGGAAGAGTTCAG-3', R: 5'-CTTGGTCTGGAGGAGACCT-3'; U6: F: 5'-GCTTCGGCAGCACATATACTAAAAT-3', R: 5'-CGCTTCAGAATTTGCGTGTCAT-3'; GAPDH: F: 5'-CGCTCTCTGCTCCTCCT-GTTC-3', R: 5'-ATCCGTTGACTC-CGACCTTCAC-3'.

Statistical Analysis

Statistical Product and Service Solutions (SPSS) 17.0 statistical software (SPSS Inc., Chicago, IL, USA) was used for all statistical analysis. Measurement data were expressed as mean ± standard deviation ($\bar{x} \pm s$). *t*-test was used to compare the difference between two groups. Count data was evaluated by χ^2 test. $p<0.05$ was considered statistically significant.

Results

Ultrasound Results of Rat Heart Examination

Compared with Sham group, LVESD and LVEDD were significantly increased in PBS group and miR-133a group, whereas left ventricular short axis shortening rate (FS) and left ventricular ejection fraction (EF) were notably decreased ($p<0.05$). Besides, compared with PBS group, LVESD and LVEDD were significantly decreased, while FS and EF were significantly increased in miR-133a group ($p<0.05$). However, they were not restored as Sham group ($p<0.05$) (Figure 1A-1D).

Myocardial Masson Staining and Collagen Volume Fraction in Rats

Masson staining of myocardial tissues showed that red cardiomyocytes were arranged neatly and tightly in sham group. A small amount of blue collagen fibers were scattered in the intercellular space (Figure 2A-a). In PBS group, a large amount of collagen fibers were found deposited in myocardial cells. Meanwhile, CVF was strikingly higher than that of Sham group ($p<0.05$) (Figure 2A-bd). On the contrary, compared with PBS group, the distribution of myocardial collagen fibers and CVF were both significantly down-regulated in miR-133a group ($p<0.05$) (Figure 2A-cd).

Immunohistochemical Detection of α-SMAL in Myocardial Tissues

In sham group, almost no α-SMA staining positive cells expressed muscle-like fibroblasts (Figure 2B-a). Meanwhile, the number of α-SMA positive cells in PBS group was significantly higher than that of sham group ($p<0.05$) (Figure 2B-b). MiR-133a significantly reduced the number of α-SMA staining positive cells in the peripheral region of MI in rats ($p<0.05$) (Figure 2B-c).

Protein Levels of Genes in Myocardial Tissues

Western blotting showed that TGF-β1, CTGF, col1 and col3 were lowly expressed in Sham group. However, the expressions of the above proteins in PBS group and miR-133a group were significantly increased when compared with Sham group ($p<0.05$). In addition, the levels of the above proteins in miR-133a group were remarkably lower than those of PBS group ($p<0.05$) (Figure 3A-3D).

Changes of Myocardial mRNA Expression in Rats

QRT-PCR results demonstrated that the expression of miR-133a in PBS group was significantly lower than that of sham operation group ($p<0.05$). The mRNA expression of miR-133a in myocardial tissues of miR-133a group was significantly higher than that of PBS group ($p<0.05$) (Figure 4A). Compared with Sham group, the mRNA expressions of TGF-β1, CTGF, col1, col3 and α-SMA in PBS and miR-133a groups were increased significantly ($p<0.05$). However, in miR-133a group, the mRNA expressions of the above genes were notably lower than those of PBS group ($p<0.05$) (Fig. 4B-4F).

Discussion

MF is a process of excessive accumulation of interstitial collagen due to disturbance of myocardial interstitial metabolism. It is also the main cause of cardiac dysfunction after MI[20]. Pathological manifestations of MF can be found in the

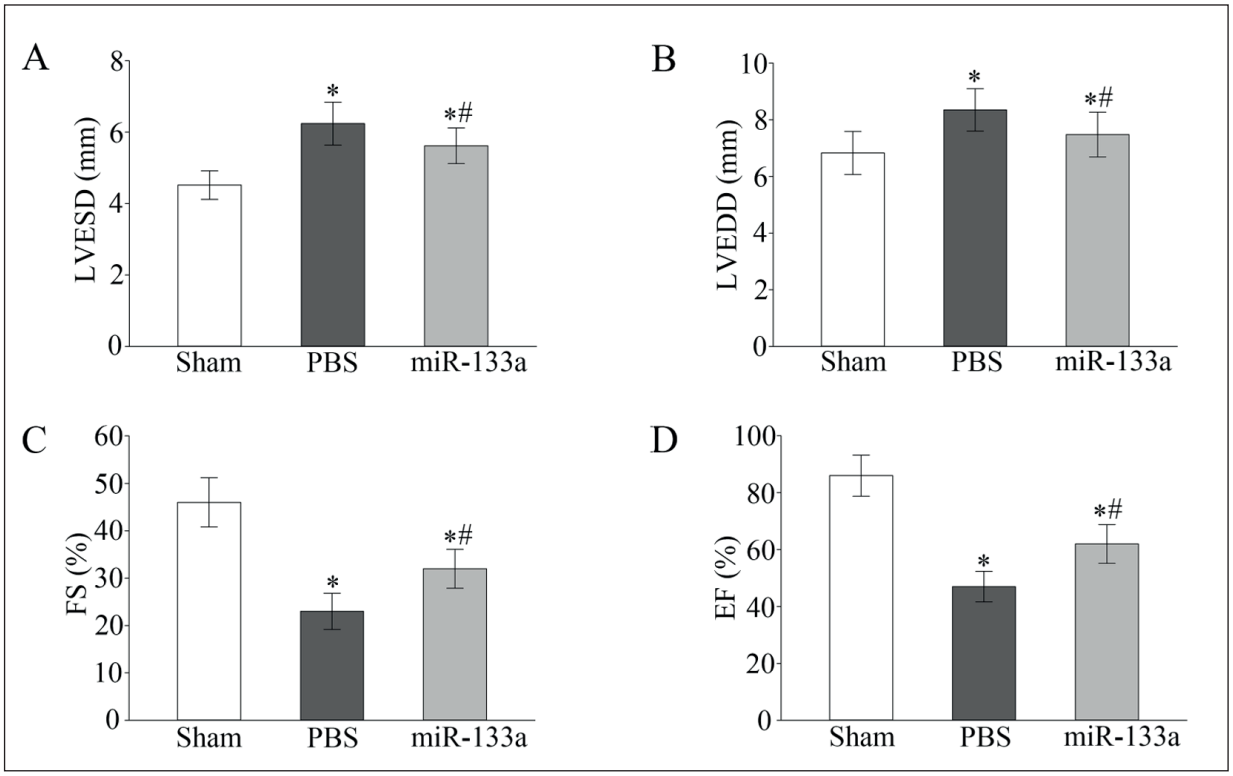

Figure 1. Cardiac function measured by color Doppler ultrasound. **A,** LVESD of rats in three groups measured by color Doppler ultrasound. **B,** LVEDD of rats in three groups measured by color Doppler ultrasound. **C,** LVFS of rats in three groups measured by cardiac color Doppler ultrasound. **D,** LVEF of rats in three groups measured by cardiac color Doppler ultrasound. *The difference was statistically significant compared with sham operation group ($p<0.05$); #Compared with control group, the difference was statistically significant ($p<0.05$).

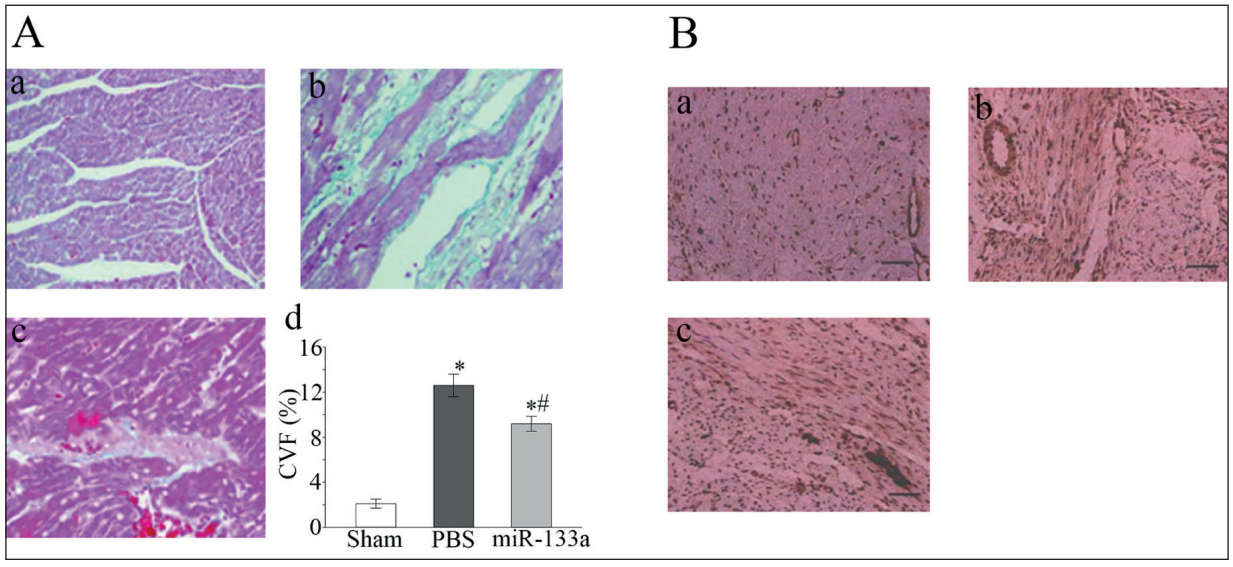

Figure 2. **A,** Masson staining and myocardial collagen volume fraction. (Magnification: 400x). **a,** Changes of MF in sham-operated rats. **b,** Changes of MF in control rats. **c,** Changes of MF in miR-133a group. **d,** Collagen volume fraction of myocardial tissue in rats of three groups measured by Masson staining. **B,** Immunohistochemical detection of rdial tissue in actirats of each group. (Magnification: 200x). **a,** Expression of α-SMA in myocardial tissue of rats in sham operation group. **b,** Expression of α-SMA in myocardial tissue of rats in control group. **c,** Expression of α-SMA in myocardial tissue of rats in miR-133a group. *The difference was statistically significant compared with sham operation group ($p<0.05$); #Compared with control group, the difference was statistically significant ($p<0.05$).

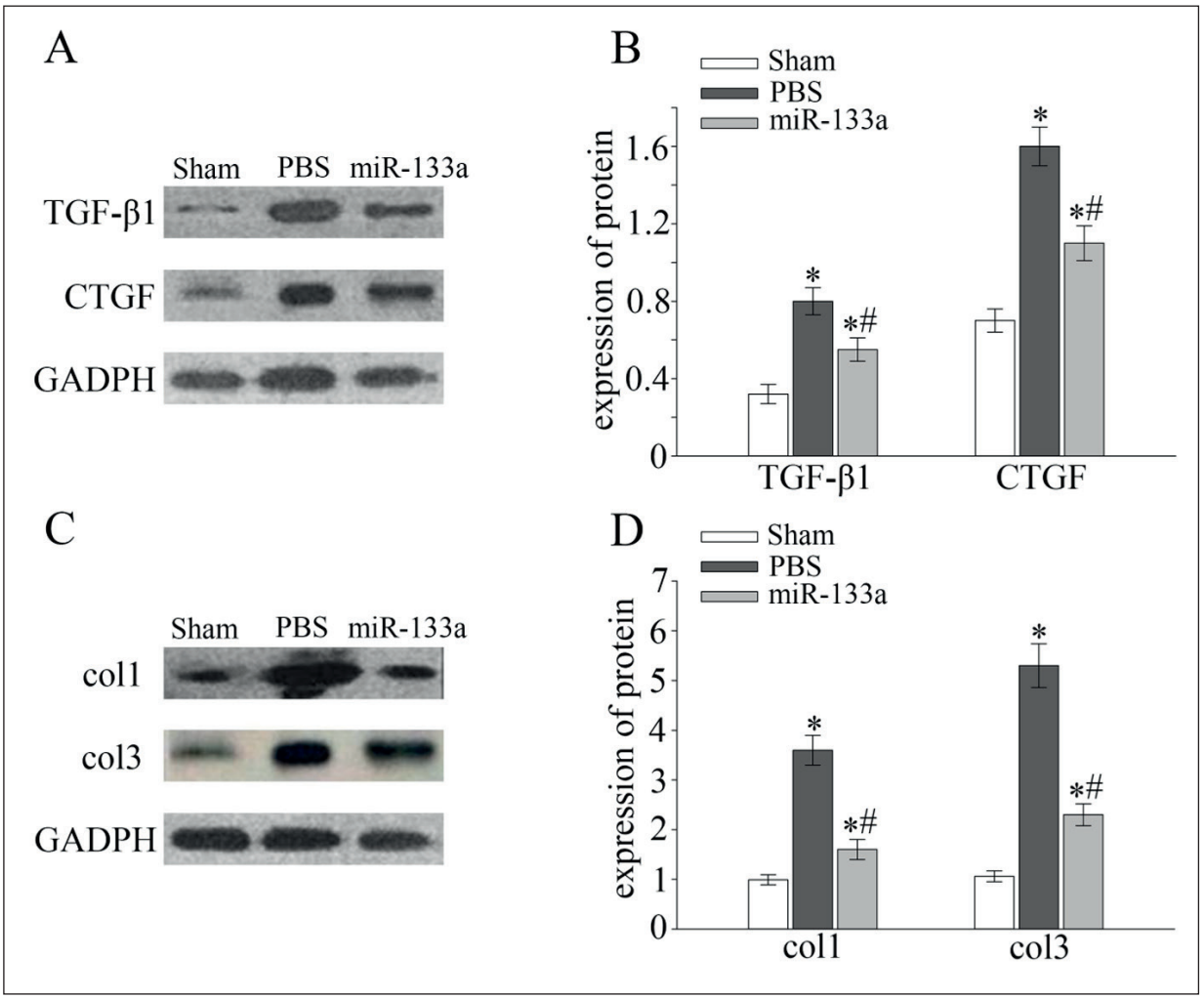

Figure 3. Immunoblotting assay for expressions of myocardial tissue-associated protein in rats of three groups**. A,** Expressions of TGF-β1 and CTGF in myocardial tissue of rats in three groups. **B,** Expressions of TGF-β1 and CTGF in myocardial tissue of rats in three groups. **C,** Expressions of col1 and col3 in myocardial tissue of rats in three groups. **D,** Expressions of col1 and col3 in myocardial tissue of rats in three groups. *The difference was statistically significant compared with sham operation group ($p<0.05$); #Compared with control group, the difference was statistically significant ($p<0.05$).

middle and late stages of various cardiovascular diseases. However, the pathogenesis of MF has not been fully clarified. Previous studies have shown that the development of MF is affected by multiple factors, including immune system, body cytokines and RAAS system. In addition, the mechanism of MF in different types is not exactly the same[21-23].

MF is characterized by excessive deposition of extracellular matrix. Myocardial interstitial cells are composed of collagen, fibronectin, proteoglycan and laminin, among which col 1 and col 3 are the main components of myocardial interstitial[24]. Among myocardial collagen, type I collagen and type III collagen account for 80-85% and 10-12%, respectively. They may together constitute a spatial structure network supporting the shape of heart. The ratio of the two collagens determines the strength and compliance of heart[25]. Under pathological conditions, changes in collagen content and composition will lead to alterations in cardiac structure and function[26]. In this research it was found that there was a small amount of collagen in myocardial cells of sham-operated group. They were mainly distributed around blood vessels, mainly type I collagen. In control group, the infarct area was thinned, and myocardial cells were significantly reduced. Meanwhile, they were replaced by a large number of structurally disor-

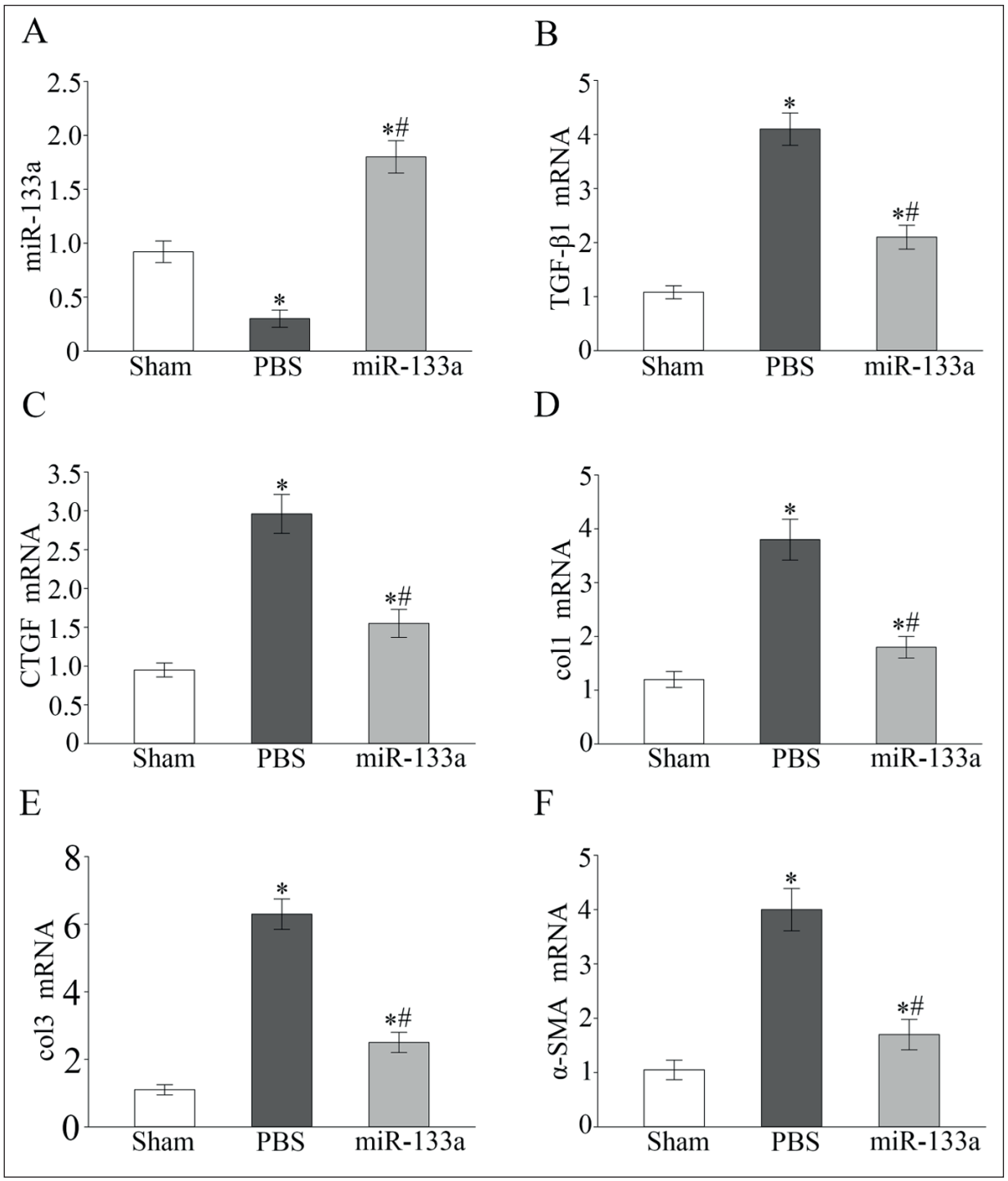

Figure 4. QRT-PCR detection of myocardial tissue-related mRNA expression levels in rats of three groups. **A,** Expression of miR-133a in myocardial tissue of rats in three groups. **B,** Expression of TGF-β1 in myocardial tissue of rats in three groups. **C,** Expression of CTGF in myocardial tissue of rats in three groups. **D,** Expression of col1 in myocardial tissue of rats in three groups. **E,** Expression of col3 in myocardial tissue of rats in three groups. **F,** Expression of α-SMA in myocardial tissue of rats in three groups. *The difference was statistically significant compared with sham operation group ($p<0.05$); #Compared with control group, the difference was statistically significant ($p<0.05$).

dered collagen fibers. Besides, myocardial cells in the infarct border zone were compensatory hypertrophy. Myocardial space was widened, and collagen fibers were deposited. Myocardial CVF and type I and III collagen levels were significantly elevated. There was a large number of inflammatory granulocytes, mononuclear cell infiltration and fibroblast proliferation as well. After 4 weeks of MI, LVEDD and LVESD were significantly increased, whereas EF and FS were markedly decreased. MiR-133a regulated the synthesis of MF-related proteins. Up-regulation of miR-133a could significantly reduce collagen fibrosis after MI. Furthermore, LVESD and LVEDD were significantly reduced, while FS and EF were significantly increased to improve cardiac function in rats. TGF-β1 plays a key role in regulating cardiac fibroblast differentiation and collagen metabolism. It promotes extracellular matrix deposition by increasing collagen and fibronectin synthesis and reducing extracellular matrix breakdown. Ultimately, this may lead to fibrosis[27]. TGF-β1 also plays a key role in the remodeling process after MI. Its overexpression may eventually lead to cardiac dysfunction[28]. In the early stage, clinical and basic experiments inhibit the fibrosis process of cardiac hypertrophy or idiopathic pulmonary fibrosis by TGF-β1 specific receptor antagonist. It has been found that inhibition of TGF-β1 can reduce the deposition of extracellular matrix and improve heart-remodeling process[29]. In healthy hearts, CTGF, a cysteine-rich growth regulator, is mainly produced by fibroblasts. When myocardial remodeling occurs, CTGF can also be secreted by cardiomyocytes[30]. As an important cytokine that maintains the progression of fibrosis, CTGF exerts many biological functions, such as promoting extracellular matrix synthesis and cell proliferation, as well as inducing cell phenotypic transformation[31, 32]. In addition, it is a key downstream factor in TGF-β1 pro-fibrotic pathway as well. Both *in vitro* and *in vivo* experiments have shown that inhibition of CTGF synthesis and activity by antisense RNA or neutralizing antibodies inhibit TGF-β1-induced collagen synthesis and fibroblast aggregation[33,34].

MiRNA is a kind of short-fragment RNA consisting of 20-23 nucleotides. MiRNA functions negatively to regulate gene expression by inhibiting mRNA transcription or mRNA degradation in the body[35]. In this work, our results showed that miR-133a expression was significantly down-regulated after MI. However, the levels of TGF-β1, CTGF, col1, col3 and α-SMA were significantly up-regulated, indicating that these changes were associated with MF after MI. In addition, overexpression of miR-133a in peripheral tissue of MI was found significantly improved cardiac function, reduced myocardial infarction area, reduced the synthesis of extracellular matrix collagen, and reduced the differentiation of cardiac fibroblasts into muscle-like fibroblasts. Meanwhile, overexpression of miR-133a significantly decreased the mRNA and protein levels of TGF-β1. This indicated that miR-133a might regulate the transcription and translation of TGF-β1. Hence, we speculated that miR-133a could regulate the expression level of TGF-β1 *via* targeting itself, thereby achieving the regulation of collagen metabolism. In conclusion, up-regulation of miR-133a attenuates MF and improves cardiac function in rats with MI. The protective effect may be due to the decrease of TGF-β1 and CTGF expression.

Conclusions

Overexpression of miR-133a down-regulates the mRNA and protein levels of TGF-β1 and CTGF after MI. Eventually, this may reduce myocardial collagen deposition, inhibit MF and improve cardiac function.

Conflict of Interest

The Authors declare that they have no conflict of interests.

References

1) Reed GW, Rossi JE, Cannon CP. Acute myocardial infarction. Lancet 2017; 389: 197-210.
2) Wang D, Zhu H, Yang Q, Sun Y. Effects of relaxin on cardiac fibrosis, apoptosis, and tachyarrhythmia in rats with myocardial infarction. Biomed Pharmacother 2016; 84: 348-355.
3) Huang DD, Huang HF, Yang Q, Chen XQ. Liraglutide improves myocardial fibrosis after myocardial infarction through inhibition of CTGF by activating cAMP in mice. Eur Rev Med Pharmacol Sci 2018; 22: 4648-4656.
4) Stratton MS, McKinsey TA. Epigenetic regulation of cardiac fibrosis. J Mol Cell Cardiol 2016; 92: 206-213.
5) Kong P, Christia P, Frangogiannis NG. The pathogenesis of cardiac fibrosis. Cell Mol Life Sci 2014; 71: 549-574.

6) Nguyen TP, Qu Z, Weiss JN. Cardiac fibrosis and arrhythmogenesis: the road to repair is paved with perils. J Mol Cell Cardiol 2014; 70: 83-91.

7) Mohr AM, Mott JL. Overview of microRNA biology. Semin Liver Dis 2015; 35: 3-11.

8) Chen C, Ponnusamy M, Liu C, Gao J, Wang K, Li P. MicroRNA as a therapeutic target in cardiac remodeling. Biomed Res Int 2017; 2017: 1278436.

9) Chen Y, Zhao Y, Chen W, Xie L, Zhao ZA, Yang J, Chen Y, Lei W, Shen Z. MicroRNA-133 overexpression promotes the therapeutic efficacy of mesenchymal stem cells on acute myocardial infarction. Stem Cell Res Ther 2017; 8: 268.

10) Liu Y, Liang Y, Zhang JF, Fu WM. MicroRNA-133 mediates cardiac diseases: mechanisms and clinical implications. Exp Cell Res 2017; 354: 65-70.

11) Diniz GP, Lino CA, Guedes EC, Moreira LN, Barreto-Chaves ML. Cardiac microRNA-133 is down-regulated in thyroid hormone-mediated cardiac hypertrophy partially via type 1 angiotensin II receptor. Basic Res Cardiol 2015; 110: 49.

12) Song T, Yao Y, Wang T, Huang H, Xia H. Tanshinone IIA ameliorates apoptosis of myocardiocytes by up-regulation of miR-133 and suppression of Caspase-9. Eur J Pharmacol 2017; 815: 343-350.

13) Castaldi A, Zaglia T, Di Mauro V, Carullo P, Viggiani G, Borile G, Di Stefano B, Schiattarella GG, Gualazzi MG, Elia L, Stirparo GG, Colorito ML, Pironti G, Kunderfranco P, Esposito G, Bang ML, Mongillo M, Condorelli G, Catalucci D. MicroRNA-133 modulates the beta1-adrenergic receptor transduction cascade. Circ Res 2014; 115: 273-283.

14) Chen X, Zhang W, Wang Q, Du L, Yi Y, Liu Y, Liu X, Duan S. Eplerenone inhibits atrial fibrosis in mutant TGF-beta1 transgenic mice. Sci China Life Sci 2016; 59: 1042-1047.

15) Zhao L, Mi Y, Guan H, Xu Y, Mei Y. Velvet antler peptide prevents pressure overload-induced cardiac fibrosis via transforming growth factor (TGF)-beta1 pathway inhibition. Eur J Pharmacol 2016; 783: 33-46.

16) Shi L, Dong N, Fang X, Wang X. Regulatory mechanisms of TGF-beta1-induced fibrogenesis of human alveolar epithelial cells. J Cell Mol Med 2016; 20: 2183-2193.

17) Yu H, Lu Y, Li Z, Wang Q. microRNA-133: expression, function and therapeutic potential in muscle diseases and cancer. Curr Drug Targets 2014; 15: 817-828.

18) Shan H, Zhang Y, Lu Y, Zhang Y, Pan Z, Cai B, Wang N, Li X, Feng T, Hong Y, Yang B. Downregulation of miR-133 and miR-590 contributes to nicotine-induced atrial remodelling in canines. Cardiovasc Res 2009; 83: 465-472.

19) Li N, Zhou H, Tang Q. miR-133: a suppressor of cardiac remodeling? Front Pharmacol 2018; 9: 903.

20) Piek A, de Boer RA, Sillje HH. The fibrosis-cell death axis in heart failure. Heart Fail Rev 2016; 21: 199-211.

21) Creemers EE, van Rooij E. Function and therapeutic potential of noncoding RNAs in cardiac fibrosis. Circ Res 2016; 118: 108-118.

22) Schuetze KB, McKinsey TA, Long CS. Targeting cardiac fibroblasts to treat fibrosis of the heart: focus on HDACs. J Mol Cell Cardiol 2014; 70: 100-107.

23) Yuan Y, Zhang Y, Han X, Li Y, Zhao X, Sheng L, Li Y. Relaxin alleviates TGFbeta1-induced cardiac fibrosis via inhibition of Stat3-dependent autophagy. Biochem Biophys Res Commun 2017; 493: 1601-1607.

24) Xiang FL, Fang M, Yutzey KE. Loss of beta-catenin in resident cardiac fibroblasts attenuates fibrosis induced by pressure overload in mice. Nat Commun 2017; 8: 712.

25) Ding Z, Yuan J, Liang Y, Wu J, Gong H, Ye Y, Jiang G, Yin P, Li Y, Zhang G, Yang C, Guo J, Chen Z, Wang X, Weng L, Zou Y. Ryanodine receptor type 2 plays a role in the development of cardiac fibrosis under mechanical stretch through TGFbeta-1. Int Heart J 2017; 58: 957-961.

26) Yuan Y, Zhang Y, Han X, Li Y, Zhao X, Sheng L, Li Y. Relaxin alleviates TGFbeta1-induced cardiac fibrosis via inhibition of Stat3-dependent autophagy. Biochem Biophys Res Commun 2017; 493: 1601-1607.

27) Guo Y, Gupte M, Umbarkar P, Singh AP, Sui JY, Force T, Lal H. Entanglement of GSK-3beta, beta-catenin and TGF-beta1 signaling network to regulate myocardial fibrosis. J Mol Cell Cardiol 2017; 110: 109-120.

28) Zhang M, Pan X, Zou Q, Xia Y, Chen J, Hao Q, Wang H, Sun D. Notch3 ameliorates cardiac fibrosis after myocardial infarction by inhibiting the TGF-beta1/Smad3 Pathway. Cardiovasc Toxicol 2016; 16: 316-324.

29) Du L, Qin M, Yi Y, Chen X, Jiang W, Zhou L, Zhang D, Xu K, Yang Y, Li C, Liu Y, Liu X, Duan SZ. Eplerenone prevents atrial fibrosis via the TGF-beta signaling pathway. Cardiology 2017; 138: 55-62.

30) Fontes MS, Kessler EL, van Stuijvenberg L, Brans MA, Falke LL, Kok B, Leask A, van Rijen HV, Vos MA, Goldschmeding R, van Veen TA. CTGF knockout does not affect cardiac hypertrophy and fibrosis formation upon chronic pressure overload. J Mol Cell Cardiol 2015; 88: 82-90.

31) Tang CM, Zhang M, Huang L, Hu ZQ, Zhu JN, Xiao Z, Zhang Z, Lin QX, Zheng XL, Yang M, Wu SL, Cheng JD, Shan ZX. CircRNA_000203 enhances the expression of fibrosis-associated genes by derepressing targets of miR-26b-5p, Col1a2 and CTGF, in cardiac fibroblasts. Sci Rep 2017; 7: 40342.

32) Chatzifrangkeskou M, Le Dour C, Wu W, Morrow JP, Joseph LC, Beuvin M, Sera F, Homma S, Vignier N, Mougenot N, Bonne G, Lipson KE, Worman

HJ, Muchir A. ERK1/2 directly acts on CTGF/CCN2 expression to mediate myocardial fibrosis in cardiomyopathy caused by mutations in the lamin A/C gene. Hum Mol Genet 2016; 25: 2220-2233.

33) Guo J, Lin Q, Shao Y, Rong L, Zhang D. miR-29b promotes skin wound healing and reduces excessive scar formation by inhibition of the TGF-beta1/Smad/CTGF signaling pathway. Can J Physiol Pharmacol 2017; 95: 437-442.

34) Dorn LE, Petrosino JM, Wright P, Accornero F. CTGF/CCN2 is an autocrine regulator of cardiac fibrosis. J Mol Cell Cardiol 2018; 121: 205-211.

35) Mohr AM, Mott JL. Overview of microRNA biology. Semin Liver Dis 2015; 35: 3-11.